Automatic Digital Modulation Recognition in the Presence of Phase Offset

Tigran A. Grigoryan, Martin Ts. Ayvazyan, and Lilit Kh. Khachatryan

Original scientific article

***Abstract*—Automatic Digital Modulation Recognition (ADMR) is a critical component in modern communication systems, enabling efficient and flexible data transmission. This paper investigates the challenges associated with ADMR in scenarios where the received signal has a phase offset. A set of features, extracted from the instantaneous amplitude and phase of the signal, is proposed for the implementation of ADMR algorithms. An artificial neural network (ANN) based recognition system is developed in the LabVIEW programming environment to classify four types of digital modulation: BPSK, QPSK, 16-QAM and 64-QAM. The simulation results indicate that the developed classifier can effectively operate in the presence of additive white Gaussian noise (AWGN) and a phase offset in the signal. The implemented ADMR algorithm achieves a recognition probability of approximately 97-99% in the signal-to-noise ratio (SNR) range of 7-30 dB for each phase offset value. The proposed ADMR algorithms achieve high recognition accuracy using fewer computational resources then other existing works.**

***Index terms*—automatic digital modulation recognition, feature extraction, phase offset, neural network.**

I. Introduction

In the real of modern communication systems, ADMR is a fundamental task for various applications, such as radio signal monitoring, intelligent communication, cognitive radio, etc. Over the years, two typical approaches have dominated the sphere of automatic modulation recognition: decision-theoretic and pattern recognition. The decision-theoretic approach uses probabilistic or likelihood functions [1] while pattern recognition uses feature-based methods [2]. Although the decision-theoretic approach can provide optimal solutions, they often involve significant computations. In contrast, a properly designed feature-based method can achieve performance similar to decision-theoretic method with significantly reduced computational complexity. The pattern recognition method divides the classification process into two components: the feature extraction subsystem and the pattern recognition subsystem. The role of feature extraction subsystem is to extract key features from the received signal, thereby reducing the amount of data processed in the pattern recognition subsystem.

In recent years, there have been many successful attempts to use an ANN in the pattern recognition subsystem [3],[4]. Asoke K. Nandi *et al* [5] proposed a three-stage recognition algorithm implemented by three feed-forward ANNs. The key features, used in the algorithm, were extracted from instantaneous amplitude, phase, and frequency of the intercepted signal, as well as from the spectrum of RF signal.

M.L.D. Wong *et al.* [6] proposed a recognition algorithm based on a set of spectral and statistical features and a feed-forward ANN. Timothy J. O'Shea *et al.* [7] proposed a recognition algorithm based on a convolutional neural network (CNN), which directly uses the baseband complex signal as input and extracts the signal characteristics to determine the modulation type.

The decision-theoretic and pattern recognition approaches have been extensively researched and have yielded valuable insights into the field. However, many existing studies and methods do not take into account the presence of phase offset in the received signals, which can lead to misclassification and reduced performance in case of real communication channels.

Jie Shi *et al*. [8] proposed a CNN-based ADMR method for BPSK, QPSK, 8-PSK and 16-QAM modulation types considering the phase offset in signal. The network directly uses in-phase and quadrature (IQ) components as input, bypassing the process of extracting the signal feature set. The proposed algorithm provides high recognition accuracy at low SNR values and the presence of a phase offset in the signal (about 92% at SNR = 5 dB). However, it requires large computational resources as the network processes raw IQ data.

Yang Liu *et al.* [9] proposed modulation recognition algorithm based on decision-theoretic approach for thirteen modulation signals: CW, AM, FM, LSB, USB, 2-ASK, 4-ASK, BPSK, QPSK, 8-PSK, 2-FSK, 4-FSK, and 16-QAM. For the recognition algorithm, the authors reused eight signal key features from [5]. These are: the maximum value of the spectral power density of the normalized-centered instantaneous amplitude (γ_{max}), the standard deviation of the direct value of the nonlinear component of the instantaneous phase (σ_{dp}), the standard deviation of the direct value of normalized instantaneous frequency (σ_{df}), the standard deviation of the absolute value of the nonlinear component of the instantaneous phase (σ_{ap}), the standard deviation of the

Manuscript received February 1, 2024; revised April 29, 2024. Date of publication May 17, 2024. Date of current version May 17, 2024. The associate editor prof. Andrej Hrovat has been coordinating the review of this manuscript and approved it for publication.

T. A. Grigoryan and L. K. Khachatryan are with the National Polytechnic University of Armenia, Armenia (e-mails: grigoryan970@gmail.com, lkhachatryan26@bk.ru).

M. T. Ayvazyan is with the State Engineering University of Armenia, Armenia (e-mail: aivazyan@mail.ru).

Digital Object Identifier (DOI): 10.24138/jcomss-2023-0189

absolute value of the normalized instantaneous frequency (σ_{af}), the standard deviation of the absolute value of the normalized centered instantaneous amplitude (σ_{aa}), the kurtosis of the normalized instantaneous amplitude (μ_{42}^{a}), and the ratio P which measures the spectrum symmetry of the RF signal. The authors determined that the 8-PSK signal could not be recognized by σ_{ap}, so they proposed a new key feature, σ_{acap}, which was calculated by further zero-centering σ_{ap}. The average accuracy of recognition results for thirteen signals is about 90% at the SNR = 8 dB. The influence of signal phase offset on the recognition accuracy has not been studied.

Yihui Wang *et al.* [10] proposed ANN based modulation recognition algorithm for the analog, digital, pulse and spread spectrum modulation types. Five frequency domain features and three high order cumulants were used in the recognition algorithm. Even though the recognition algorithm covers many modulation schemes, the recognition accuracy is low at SNR = 15 dB and below (about 92% at SNR = 15 dB). The influence of signal phase offset on the recognition accuracy has not been studied.

Mingqian Liu *et al.* [11] proposed ADMR algorithm that uses decision thresholds for the recognition of BPSK, QPSK and 8-PSK modulation types. The decision thresholds were calculated based on analysis of the cyclostationarity and cyclic spectrum of signal. The proposed method achieves a prediction accuracy of about 88-95% at SNR = 7 dB, across various phase offset values. The research focused only on the intra-class recognition (M-PSK modulation).

Kai Liu *et al.* [12] proposed a multiscale convolution-based network model (MSNet-SF) for the recognition of eight digital modulation schemes: BPSK, QPSK, 8-PSK, 4-PAM, 16-QAM, 64-QAM, GFSK, CPFSK. The input of the network is 4096x2 IQ data, $C_{40}, C_{42}, C_{63}, C_{80}$ high order cumulants and the kurtosis of the normalized instantaneous amplitude μ_{42}^{a}. The proposed ADMR method gives prediction accuracy of about 95%, 90%, 75%, 85% at SNR = 7 dB for BPSK, QPSK, 16-QAM, 64-QAM modulation types, respectively. The influence of signal phase offset on the recognition accuracy has not been studied and the proposed method requires large computational resources

In this paper, an ADMR system is proposed that can operate effectively in the presence of AWGN and phase offset in the signal. It requires less computational resources compared to the other methods. The pattern recognition approach was chosen, and a set of seven instantaneous time-domain features was proposed for implementing automatic recognition algorithms for four types of digital modulations: BPSK, QPSK, 16-QAM and 64-QAM. A multilayer perceptron or feed-forward backpropagation neural network was used as a classifier in the pattern recognition subsystem.

The paper is organized as follows. This introduction is followed by section II, which details the architecture and hyperparameters of proposed ANN used for the ADMR. Next, section III describes the signal model used for the investigation of the ADMR problem. Section IV describes the extraction of the signal features set used for the training of the ANN and recognition of four digital modulation types. Section V is dedicated to presenting the test results and is followed by the conclusion.

II. ANN Architecture and Hyperparameters

Each ANN consists of input, output and hidden layers. The proposed signal feature set is used as input to the ANN. Since the set contains seven features, the input layer of the ANN must contain seven neurons. The output layer of the ANN is determined based on the number of modulation types that need to be classified. Accordingly, the output layer of the network contains four neurons, each of which represents one of the modulation types examined in this paper. The optimal number of hidden layers and neurons was determined during the experiments.

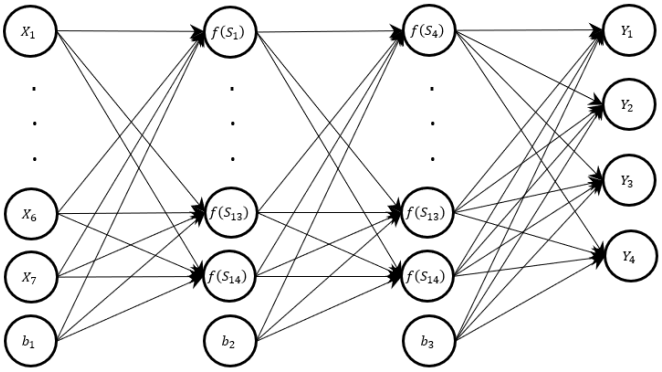

Fig. 1. The proposed ANN architecture for the ADMR problem.

Based on the experimental results, the ANN architecture with two hidden layers was chosen, with each layer containing fourteen neurons. Given that the training duration of the ANN with this architecture was relatively short (approximately 10 minutes) compared to more complex architectures with additional hidden layers or neurons, and considering its comparable recognition accuracy, it was identified as optimal for the ADMR problem under consideration. The proposed ANN architecture also contains bias neurons in each layer except the output one (Fig. 1). This is a special type of neuron that has a constant value and is not connected to the neurons of the previous layer. The inclusion of bias neurons enables the adjustment of the activation function by shifting it to the left or right.

In this paper, the backpropagation method [13] was chosen to train the ANN. This method propagates the error value from the network outputs to its inputs to adjust the weights of the neurons:

$$w_{i,j} = w_{i,j} + \Delta w_{i,j} \tag{1}$$

where $w_{i,j}$ is the weight of the synapse connecting the neurons i and j, and $\Delta w_{i,j}$ is the value with which the synapse weight needs to be updated.

The backpropagation algorithm uses the gradient descent method to update the weights of the neurons [14]. The $\Delta w_{i,j}$ is defined as follows:

$$\Delta w_{i,j} = \eta \delta_j \frac{df(S_j)}{dS} f(S_i) \quad (2)$$

where η is the learning rate, δ_j is the loss value of the j-th neuron, S_j is the state of the j-th neuron, $f(S_j)$ is the value of the activation function of the j-th neuron and $f(S_i)$ is the value of the activation function of the i-th neuron.

The sigmoid function is used as the activation function of neurons in the network:

$$f(x) = \frac{1}{1 + e^{-x}} \quad (3)$$

Equation (2) clarifies that the learning rate is associated with the magnitude of the gradient step that is used to update the weights of the network.

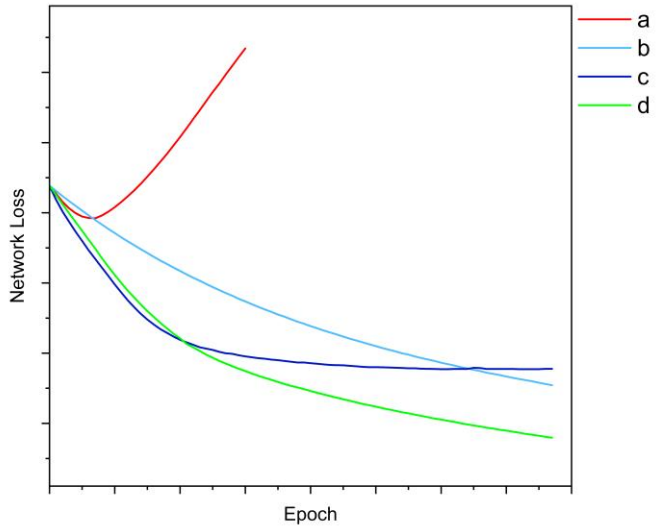

Fig. 2. The influence of learning rate on network loss.
a) learning rate is much too high, b) learning rate is too low, c) learning rate is high, d) learning rate is optimal

The choice of the learning rate is crucial for the performance of the neural network. Inappropriate selection of this hyperparameter can result in extended training time or in extreme cases make it impossible to train the network (Fig. 2).

There are many different methods for learning rate value control. In this paper, the cyclic change method [15] is chosen to control the learning rate during network training. In this method, the learning rate graph varies between the low and high thresholds. During these variations in the learning rate, the error value has the potential to move away from the sharp minima in the network loss graph. Although this might result in a temporary increase in network loss, it could eventually facilitate convergence towards more desirable minima of the network loss graph [16].

Various adaptations of this method exist. For example, during one cycle, the learning rate can decrease and increase linearly or exponentially. In addition, after each cycle, also the value of the upper threshold can decrease linearly or exponentially (Fig. 3).

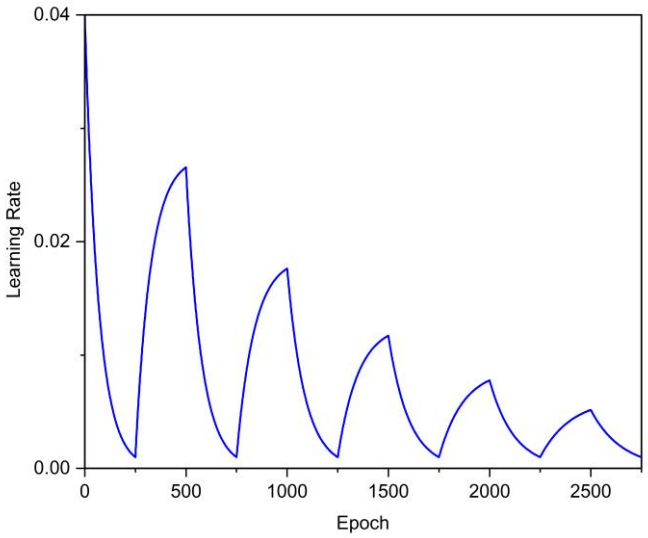

Fig. 3. Example of a cyclic learning rate with exponential decay

III. Signal Model

To build up a working model of the system, we assume that the carrier frequency and symbol timing of the signal are known apriori, the transmitted signal has passed through the AWGN channel and phase offset has been added to the signal as the effect of non-ideal synchronization.

In accordance with this, the received signal model can be represented by the following equation:

$$s(t) = m(t) + g(t) \quad (4)$$

where, $m(t)$ is considered as the modulated signal and $g(t)$ is an AWGN.

The modulated signal $m(t)$ can be written as:

$$m(t) = Re\{\alpha \dot{m}_e(t) e^{j2\pi f_c t} e^{j\varphi_c}\} \quad (5)$$

where, $\dot{m}_e(t)$ is the complex envelope of the modulated signal, α is the channel attenuation factor, f_c is the carrier frequency, φ_c is the phase offset and $Re\{.\}$ denotes the real part. It is considered that phase offset, and the attenuation factor are constant at the same observation period.

The complex envelope $\dot{m}_e(t)$ can be written as:

$$\dot{m}_e(t) = I(t) + jQ(t) = a(t) e^{j\varphi(t)} \quad (6)$$

where, $I(t)$ is the in-phase component, $Q(t)$ is the quadrature component, $a(t)$ is the amplitude and $\varphi(t)$ is the phase of the baseband signal.

For the future feature extraction, we will use a simulated baseband signal that is affected by AWGN and phase offset. Considering the fact that the amplitude of the baseband signal may vary in different channels due to the attenuation factor of the channel, it is necessary to normalize the amplitude of the signal. Since the signal contains a zero mean AWGN,

normalization should be performed using the mean of the signal amplitude:

$$a_n(t) = a(t)/\mu_{a(t)} \tag{7}$$

where, $\mu_{a(t)}$ is the mean of the signal amplitude.

IV. Feature Extraction

The most commonly used signal features in the ADMR can be divided into two types: instantaneous time domain [17],[18] and statistical [19], [20], [21]. Instantaneous time domain features are calculated based on the instantaneous amplitude, phase, and frequency of the signal. Statistical features are extracted using higher-order moments, higher-order cumulants, and higher-order cyclic cumulants. Some studies also use these two types of features together for ADMR algorithms [22].

The feature set, used in this paper, was calculated based on the instantaneous amplitude and instantaneous phase of the simulated signal. The feature set proposed in [5] serves as the foundation for many studies that utilize instantaneous time domain features for the ADMR algorithms. In this paper, one feature is reused and two others are modified from the key feature set proposed in [5]. The reused feature is the standard deviation of the absolute value of the centered non-linear component of the instantaneous phase (σ_{pcnl}). The two other features represent modified versions of the σ_{aa} and μ_{42}^{a} features. In addition to these three features, four new features are proposed. The complete feature set proposed for the recognition of BPSK, QPSK, 16-QAM, and 64-QAM modulations consists of seven key features.

The proposed features, that are calculated based on the instantaneous amplitude, are defined as follows:

The standard deviation of the normalized instantaneous amplitude:

$$\sigma_{an} = \sqrt{\frac{\sum(a_n(i) - \mu_{an})^2}{n-1}} \tag{8}$$

where n is the number of samples and μ_{an} is the mean of the normalized instantaneous amplitude (equal to 1).

The skewness of the normalized instantaneous amplitude:

$$S_{an} = \frac{\sum(a_n(i) - \mu_{an})^3}{n\,{\sigma_{an}}^3} \tag{9}$$

The mean of the absolute value of the normalized centered instantaneous amplitude:

$$\mu_{anc} = \frac{1}{n}\sum|a_{nc}(i)| \tag{10}$$

where $a_{nc}(i)$ is the normalized centered instantaneous amplitude and is defined as follows:

$$a_{nc}(i) = a_n(i) - 1 \tag{11}$$

The skewness of the absolute value of the normalized centered instantaneous amplitude:

$$S_{anc} = \frac{\sum(|a_{nc}(i)| - \mu_{anc})^3}{n\,{\sigma_{anc}}^3} \tag{12}$$

where σ_{anc} is the standard deviation of the absolute value of the normalized centred instantaneous amplitude.

The kurtosis of the absolute value of the normalized centered instantaneous amplitude:

$$K_{anc} = \frac{\sum\left(|a_{nc}(i)| - \mu_{a_{nc}}\right)^4}{n\,{\sigma_{anc}}^4} \tag{13}$$

The proposed features, that are calculated based on the instantaneous phase, are defined as follows:

The mean of the absolute value of the centered non-linear component of the instantaneous phase:

$$\mu_{pcnl} = \frac{1}{n}\sum|\varphi_{cnl}(i)| \tag{14}$$

where $\varphi_{cnl}(i)$ is the centered non-linear component of the instantaneous phase.

The standard deviation of the absolute value of the centered non-linear component of the instantaneous phase:

$$\sigma_{pcnl} = \sqrt{\frac{1}{n}\left[\sum\varphi_{cnl}^2(i)\right] - \left[\frac{1}{n}\sum|\varphi_{cnl}(i)|\right]^2} \tag{15}$$

In order to evaluate the proposed signal key features, a set of 100 signals for each modulation type was simulated using the LabVIEW programming environment. Each simulated signal contained 4096 random symbols, with each symbol containing 8 samples. The instantaneous amplitude and phase of these signals were subsequently extracted. Based on these parameters, the values of signal key features were calculated. The key feature values for an SNR of 7 dB are shown in Figs. 4-10.

The features calculated from the instantaneous amplitude of the signal can be used to classify 16-QAM and 64-QAM modulation types.

From Figs. 4-8, it is clear that 16-QAM and 64-QAM modulations can be differentiated from each other by the set of features σ_{an}, S_{an}, μ_{anc}, S_{anc} and K_{anc}. In M-QAM modulations, both the phase and amplitude of the signal are being changed. As the number of possible amplitude values for 16-QAM differs from that of 64-QAM modulation, the values of key features, calculated based on the instantaneous amplitude of the signal, remain in different regions. However, the classification of the QPSK and BPSK modulation types cannot be achieved with these five features. In these modulations, only the phase of the signal changes and they each have only one absolute amplitude value. That amplitude value is identical for both QPSK and BPSK.

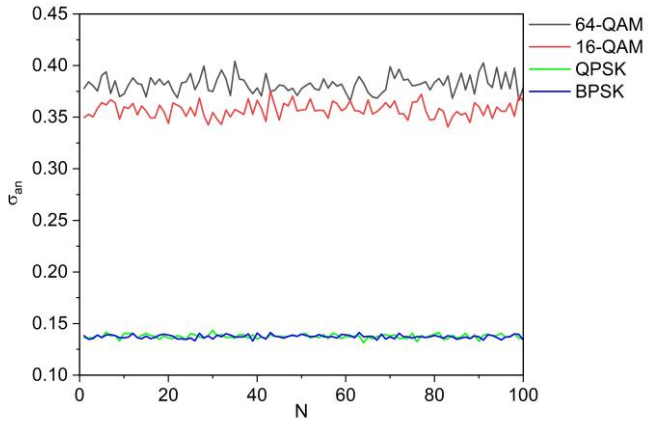

Fig. 4. The value of σ_{an} for 100 simulated 64-QAM, 16-QAM, QPSK and BPSK signals at SNR = 7 dB; N = 1,2,…,100 represents the number of the simulated signal (e.g. when N = 20, it refers to the 20th simulated signal)

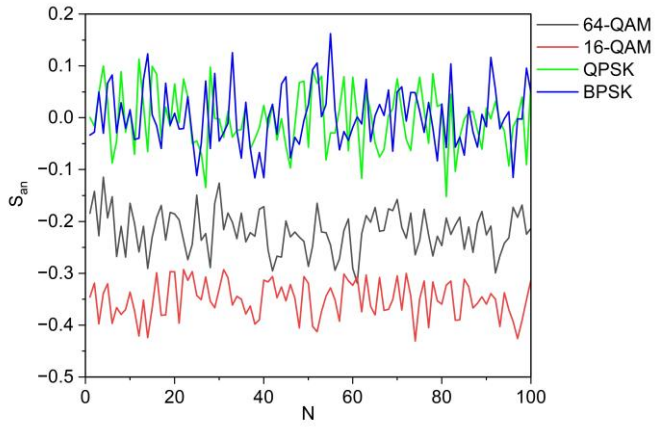

Fig. 5. The value of S_{an} for 100 simulated 64-QAM, 16-QAM, QPSK and BPSK signals at SNR = 7 dB; N = 1,2,…,100 represents the number of the simulated signal (e.g. when N = 20, it refers to the 20th simulated signal)

From Figs. 4-8, it is clear that 16-QAM and 64-QAM modulations can be differentiated from each other by the set of features σ_{an}, S_{an}, μ_{anc}, S_{anc} and K_{anc}. In M-QAM modulations, both the phase and amplitude of the signal are being changed. As the number of possible amplitude values for 16-QAM differs from that of 64-QAM modulation, the values of key features, calculated based on the instantaneous amplitude of the signal, remain in different regions. However, the classification of the QPSK and BPSK modulation types cannot be achieved with these five features. In these modulations, only the phase of the signal changes and they each have only one absolute amplitude value. That amplitude value is identical for both QPSK and BPSK.

The features calculated from the instantaneous phase of the signal (μ_{pcnl} and σ_{pcnl}) can be used to classify QPSK and BPSK modulation types (Figs. 9-10).

However, the classification of the 16-QAM and 64-QAM modulation types cannot be achieved with these two features. 16-QAM and 64-QAM modulations have many possible phase values, and the differences between these values are much smaller compared to those in BPSK and QPSK modulations.

As a result, in the case of low SNR values, the key feature values calculated based on the instantaneous phase of the signal for 16-QAM and 64-QAM start to overlap in their respective regions.

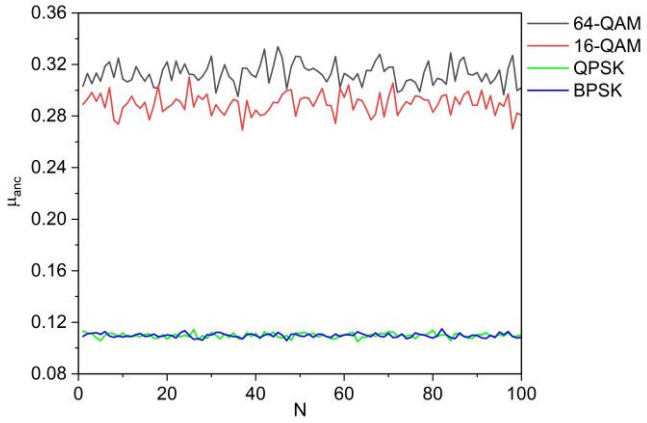

Fig. 6. The value of μ_{anc} for 100 simulated 64-QAM, 16-QAM, QPSK and BPSK signals at SNR = 7 dB; N = 1,2,…,100 represents the number of the simulated signal (e.g. when N = 20, it refers to the 20th simulated signal)

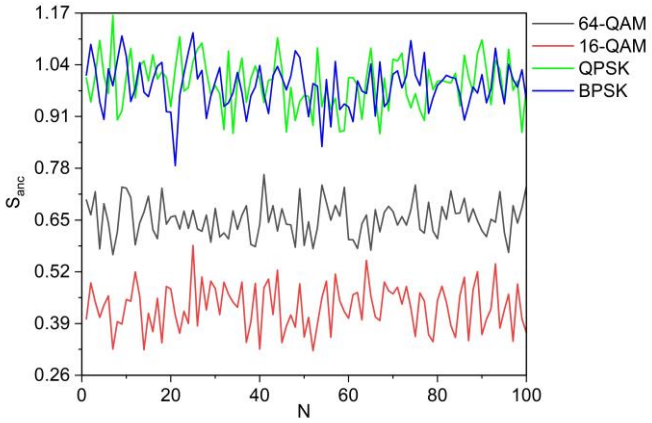

Fig. 7. The value of S_{anc} for 100 simulated 64-QAM, 16-QAM, QPSK and BPSK signals at SNR = 7 dB; N = 1,2,…,100 represents the number of the simulated signal (e.g. when N = 20, it refers to the 20th simulated signal)

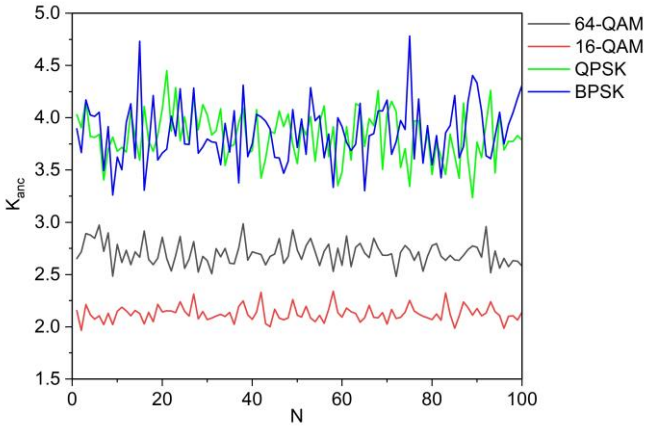

Fig. 8. The value of K_{anc} for 100 simulated 64-QAM, 16-QAM, QPSK and BPSK signals at SNR = 7 dB; N = 1,2,…,100 represents the number of the simulated signal (e.g. when N = 20, it refers to the 20th simulated signal)

Intra-class recognition of M-PSK modulations can be achieved through key features extracted from the instantaneous phase of the signal. Similarly, for M-QAM modulations, intra-class recognition can be achieved by using key features calculated from the instantaneous amplitude of the signal. However, the inter-class recognition between M-PSK and M-QAM modulations can only be achieved by combining the seven key features described above.

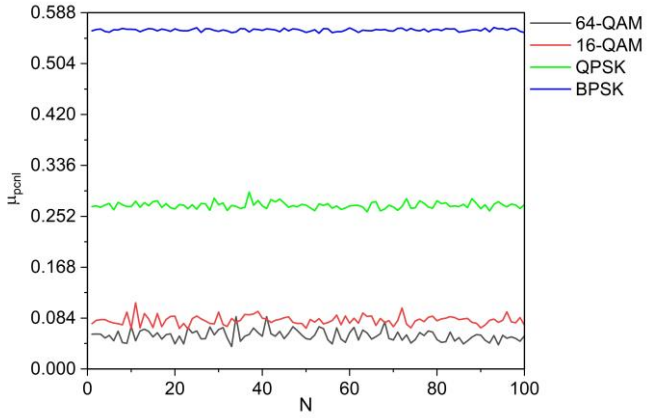

Fig. 9. The value of μ_{pcnl} for 100 simulated 64-QAM, 16-QAM, QPSK and BPSK signals at SNR = 7 dB; N = 1,2,…,100 represents the number of the simulated signal (e.g. when N = 20, it refers to the 20th simulated signal)

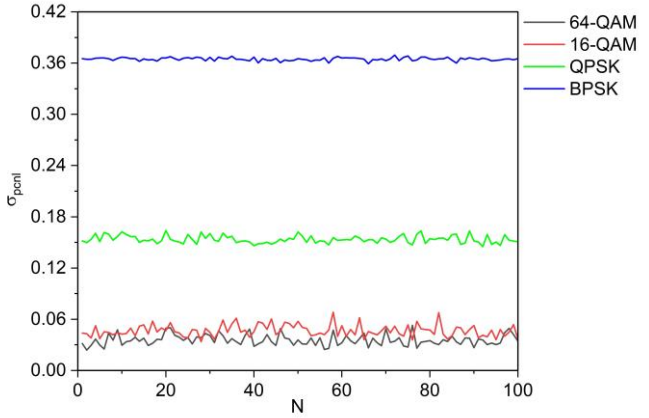

Fig. 10. The value of σ_{pcnl} for 100 simulated 64-QAM, 16-QAM, QPSK and BPSK signals at SNR = 7 dB; N = 1,2,…,100 represents the number of the simulated signal (e.g. when N = 20, it refers to the 20th simulated signal)

The phase offset of the signal affects only two features from the set described above, μ_{pcnl} and σ_{pcnl}. Despite this, these features are still applicable for ADMR. This is because the values of these features for QPSK and BPSK modulation types fall within distinct ranges (without any overlap) and can be differentiated throughout the complete cycle of the phase offset (Fig.11-12). As the phase offset doesn't have an impact on the key features calculated from the instantaneous amplitude of the signal, the recognition of 16-QAM and 64-QAM modulations in the presence of phase offset in the signal can still be achieved by using key features σ_{an}, S_{an}, μ_{anc}, S_{anc} and K_{anc}.

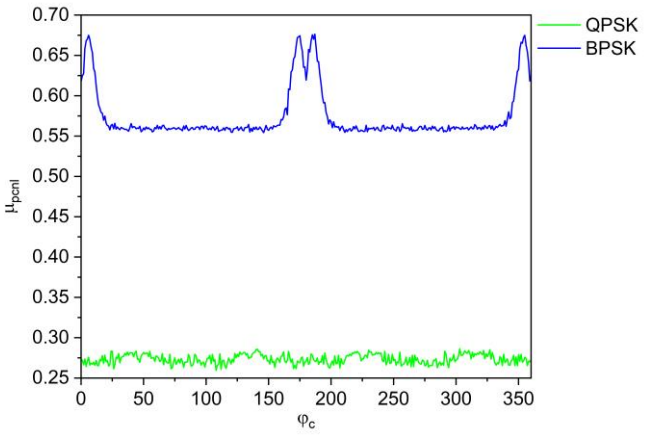

Fig. 11. The value of μ_{pcnl} against phase offset φ_c for QPSK and BPSK signals at SNR=7 dB

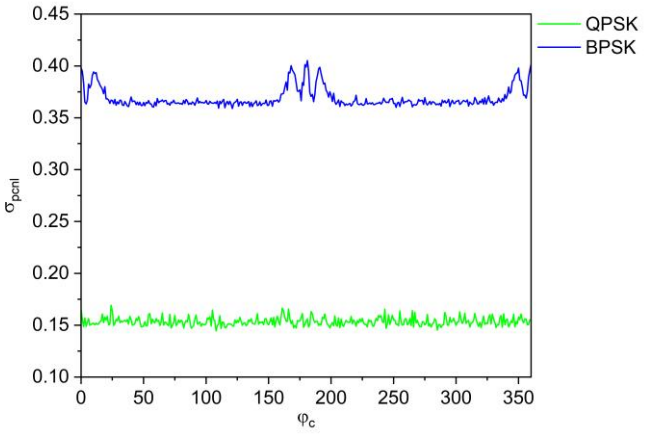

Fig. 12. The value of σ_{pcnl} against phase offset φ_c for QPSK and BPSK signals at SNR=7 dB

V. Experimental Results

Described ADMR algorithms were implemented in the LabVIEW programming environment. For each modulation type, 500 baseband signals were generated with a random SNR in the range of 6-30 dB and a random phase offset in the range of 0-45 degrees.

Experiments have demonstrated that the network training process becomes significantly challenging when the lower limit of the SNR for the generated signals is 5 dB or less. Even if the network was trained on such data, classification of the 16-QAM and 64-QAM modulated signals with SNR = 5 dB or lower becomes impossible. The network treats them as the same modulation type and gives a recognition probability of about 99% for one of them and a recognition probability of about 0-1% for the other. This happens because the values of the key features, calculated to classify the 16-QAM and 64-QAM signals, start to overlap each other at the SNR value of 5 dB and lower (Fig.13). Because of this, the decision was made to train the network using signals with SNR in the range of 6-30 dB.

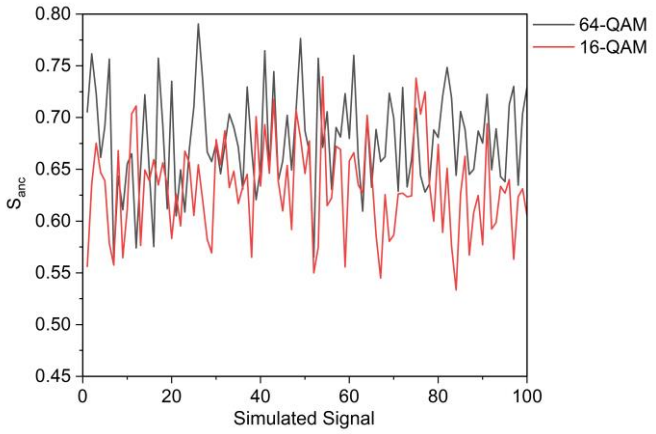

Fig. 13. The value of S_{anc} for 100 simulated 64-QAM and 16-QAM signals at SNR = 5 dB

The phase offset range was selected to be 0-45 degrees, as the value of μ_{pcnl} within this range encompasses all the values present throughout a complete phase offset cycle (Fig.11). By training the ANN with this range, all phase offset values will be covered.

During the training process, the cyclic change control method with an exponential decay of epochs and cycles was used for the learning rate control (Fig. 3).

After each epoch, the root mean square error of the network was calculated, and if it was less than 0.01, then the network was considered as trained:

$$\delta_{RMS} = \sqrt{\frac{\sum \left(\frac{\sum \delta_m}{m}\right)^2}{n}} \tag{16}$$

where m is the count of output neurons, δ_m is the error value of the m-th output neuron and n is the size of the training data.

TABLE I
RECOGNITION RESULTS

	6 dB	7 dB	10 dB	15 dB	20 dB	30 dB
BPSK	97.94%	97.79%	97.35%	97.41%	98.15%	98.17%
QPSK	91.51%	97.08%	99.44%	99.54%	99.55%	99.55%
16-QAM	32.59%	99.03%	99.11%	99.14%	99.15%	99.15%
64-QAM	99.1%	99.15%	99.17%	98.9%	98.81%	98.89%

For the recognition test, 1000 signals were generated for each modulation type at the specified SNR value. The phase offset dynamically changed, starting from 0 degrees and increasing by one degree with each generated signal. Within the same observation period the phase offset remained constant. At the end, the average recognition probability was calculated. The results of the recognition test are presented in Table 1.

At SNR = 6 dB, the recognition probability of 16-QAM modulation drops sharply to ~30%, but the network is still able to classify BPSK and QPSK modulations with high probability (Table I.).

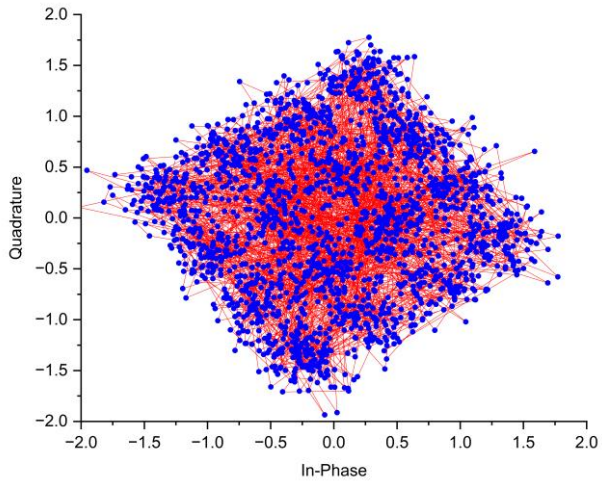

Fig. 14. The constellation of generated 16-QAM signal at SNR = 6 dB and φ_c = 35°

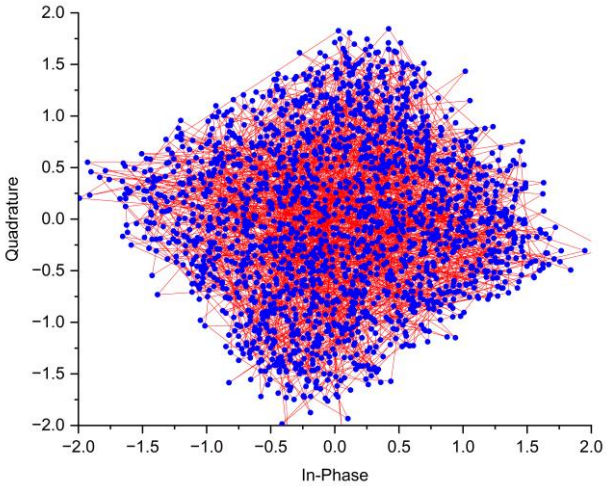

Fig. 15. The constellation of generated 64-QAM signal at SNR = 6 dB and φ_c = 35°

The high recognition probability for 64-QAM modulation, coupled with the low recognition probability for 16-QAM modulation at SNR = 6 dB, indicates that the network is not able to classify 16-QAM and 64-QAM modulations at this SNR value (Fig.14, Fig.15). For the SNR values greater than 6 dB, the network classifies all examined modulation types with a high recognition probability, regardless of the phase offset value.

VI. CONCLUDING REMARKS

In this paper, the automatic recognition of four types of digital modulation in the presence of both phase offset and AWGN was studied. A set of seven signal key features (σ_{an}, S_{an}, μ_{anc}, S_{anc}, K_{anc}, μ_{pcnl} and σ_{pcnl}) for the ADMR problem was proposed. It was shown that BPSK and QPSK modulation types can be classified using the features μ_{pcnl} and σ_{pcnl}. Similarly, 16-QAM and 64-QAM can be classified using the features σ_{an}, S_{an}, μ_{anc}, S_{anc} and K_{anc}.

To study the performance of this feature set, an ANN architecture was proposed and implemented in the LabVIEW programming environment.

The proposed ADMR algorithms give ability to classify BPSK, QPSK, 16-QAM and 64-QAM modulation types with a high recognition probability (about 97-99%) at SNR range of 7-30 dB and at all phase offset values. Compared to other existing works, the proposed ADMR algorithms achieve high recognition accuracy using fewer computational resources.

In future studies, the key feature set could be expanded to enhance the network's ability to classify additional modulation types. Additionally, the impact on recognition accuracy of both dynamically changing phase offset during the same observation period and frequency offset could be investigated.

REFERENCES

[1] J. L. Xu, Su Wei, Z. Mengchu, "Likelihood-Ratio Approaches to Automatic Modulation Classification", IEEE Transactions on Systems, Man and Cybernetics, Part C: Applications and Reviews, vol.41, pp.455-469, 2011.

[2] O. A. Dobre, A. Abdi, Y. Bar-Ness, and W. Su, "Survey of automatic modulation classification techniques: Classical approaches and new trends," IET Comm., vol. 1, pp. 137-156, 2007.

[3] Salah Ayad Jassim and Ibrahim Khider, "Comparison of Automatic Modulation Classification Techniques," Journal of Communications vol. 17, no. 7, pp. 574-580, July 2022.

[4] S. Xie and J. Ye, "Overview of Automatic Modulation Recognition Methods," 2023 International Conference on Distributed Computing and Electrical Circuits and Electronics (ICDCECE), Ballar, India, 2023, pp. 1-7.

[5] A. K. Nandi, and E. E Azzouz, "Algorithms for Automatic Modulation Recognition of Communication Signals," IEEE Trans. Commun., vol. 46, pp. 431-436, 1998.

[6] M. L. D. Wong, A.K. Nandi, Automatic digital modulation recognition using spectral and statistical features with multi-layer perceptrons, In Proceedings of International Symposium of Signal Processing and Application (ISSPA), Kuala Lumpur, Vol. II, 2001, pp. 390 –393.

[7] O'Shea, T.J. Corgan, J. Clancy, T.C. Convolutional Radio Modulation Recognition Networks. In Proceedings of the Communications in Computer and Information Science, Aberdeen, UK, 2–5 September 2016, Springer: Cham, Switzerland, 2016, pp. 213–226.

[8] J. Shi, S. Hong, C. Cai, Y. Wang, H. Huang and G. Gui, "Deep Learning-Based Automatic Modulation Recognition Method in the Presence of Phase Offset," in IEEE Access, vol. 8, pp. 42841-42847, 2020.

[9] Y. Liu, D. Xu, W. Xu, H. Wang, X. Li and L. Qi, "An algorithm of modulated signal recognition based on statistical parameters," 2022 IEEE 10th Asia-Pacific Conference on Antennas and Propagation (APCAP), Xiamen, China, 2022, pp. 1-2.

[10] Y. Wang, Z. Liu and Y. Xu, "Application of frequency-domain features and high-order cumulants in ANN-based communication modulation recognition," 2022 IEEE 4th International Conference on Civil Aviation Safety and Information Technology (ICCASIT), Dali, China, 2022, pp. 1288-1293.

[11] M. Liu, Z. Wen, Y. Chen and M. Li, "Modulation recognition with frequency offset and phase offset over multipath channels," in China Communications, vol. 20, no. 10, pp. 58-69, Oct. 2023.

[12] K. Liu and F Li, "Automatic modulation recognition based on a multiscale network with statistical features", Physical Communication, pp. 102052, 2023.

[13] G. Bebis, M. Georgiopoulos, Feed-forward neural networks. Potentials IEEE, 1994, vol. 13, pp. 27 – 31.

[14] P. Baldi, "Gradient descent learning algorithm overview: A general dynamical systems perspective," IEEE Trans. Neural Netw., vol. 6, no. 1, pp. 182-195, Jan. 1995.

[15] L. N. Smith, "Cyclical learning rates for training neural networks", in IEEE Winter Conference on Applications of Computer Vision, 2017, pp. 464–472.

[16] T. A. Grigoryan, "Research of Neural Network Learning Rate Control Methods for The Automatic Signal Type Recognition", Armenian Journal of Physics, 2021, vol. 14, issue 2, pp. 91-98.

[17] J. J. Popoola, R. van Olst, "A Novel Modulation-Sensing Method," IEEE Vehicular Tech. Mag., vol.6, no.3, pp.60-69, Sept. 2011.

[18] S. Ansari, K. A. Alnajjar, S. Abdallah, and M. Saad, ''Automatic digital modulation recognition based on machine learning algorithms,'' in Proc. Int. Conf. Commun., Comput., Cybersecur., Informat. (CCCI), Nov. 2020, pp. 1–6.

[19] A. Swami and B. M. Sadler, ''Hierarchical digital modulation classification using cumulants,'' IEEE Trans. Commun., vol. 48, no. 3, pp. 416–429, Mar. 2000.

[20] V. D. Orlic and M. L. Dukic, "Automatic modulation classification algorithm using higher-order cumulants under real-world channel conditions," IEEE Commun. Lett., vol. 13, no. 12, pp. 917–919, Dec. 2009.

[21] M. Pedzisz and A. Mansour, "Automatic modulation recognition of MPSK signals using constellation rotation and its 4th order cumulant," Digit. Signal Prog., vol. 15, no. 3, pp. 295-304, May 2005.

[22] W. Juan-ping, H. Ying-zheng, Z. Jin-mei, and W. Hua-kui. Automatic modulation recognition of digital communication signals. In 2010 First International Conference on Pervasive Computing, Signal Processing and Applications, pages 590–593, Sep. 2010.

Tigran A. Grigoryan was awarded the B.S and M.S. degrees in Radio Engineering and Communications by National Polytechnic University of Armenia, Yerevan, Armenia, in 2019 and 2021 respectively. He is currently pursuing the Ph.D. degree in Communication Systems at National Polytechnic University of Armenia, Yerevan, Armenia.

From 2018-2019 he was a R&D Engineer at YEA Engineering, Yerevan, Armenia. From 2019-2020 he was a Solution Engineer at National Instruments, Yerevan, Armenia. From 2020-2022 he was a Staff Solution Engineer at NI, Yerevan, Armenia. Currently, he is a Senior Solution Engineer at NI, Yerevan, Armenia.

His research interests include digital signal processing and radar systems.

His work includes the development of test systems for the Advanced Driver Assistance Systems (ADAS).

Martin Ts. Aivazyan was awarded the M.S. degree in Radio Engineering by Institute of Radio Physics and Electronics of the Armenian Academy of Science, Yerevan, Armenia, in 1979 and the Ph.D. degree in Radio Electronics by the Institute of Radiotechnics and Electronics of Academy of Sciences, Moscow, Russia, in 1985 and in 2020 Doctor of Technical Sciences (Engineering) by National Polytechnic University of Armenia.

From 1982 to 1990, he was a senior scientific worker at the Institute of Radio Physics and Electronics of Armenian Academy of Sciences, Yerevan, Armenia. Currently he is an Professor and the Head of 5G Research Group at the Institute of IT and Electronics, National Polytechnic University of Armenia, Yerevan, Armenia. His research interests include mmWave communications, RF component design and mobile communications.

Lilit Kh. Khachatryan was awarded the M.S. degree in Radio Engineering by Institute of Radio Physics, Yerevan, Armenia, in 2008 and the Ph.D. degree in of Technical Sciences (Engineering) by the National Polytechnic University of Armenia, Yerevan, in 2015. From 1989 to 2002, she was a senior scientific worker at the Scientific Research Institute of Radiophysics, Yerevan, Armenia. Currently she is an Associate Professor at the National Polytechnic University of Armenia, Yerevan, Armenia. Her research interests include measurements of antenna parameters in the near field, RF component design and mobile communications.